Mediated Coadsorption at the Liquid−Solid Interface: Stabilization through Hydrogen Bonds

Lorenz Kampschulte,[†] Stefan Griessl,[†] Wolfgang M. Heckl,[†,‡] and Markus Lackinger*[,†]

Ludwig-Maximilians-University Munich, Department for Earth- and Environmental Sciences, and Center for Nanoscience (CeNS), Theresienstr. 41, 80333 München, Germany, and Deutsches Museum, Museumsinsel 1, 80538 München, Germany

Received: February 15, 2005; In Final Form: March 31, 2005

Stable adsorption of 1,3,5-tris(4-pyridyl)-2,4,6-triazine (TPT) molecules from the liquid phase was only observed in binary solutions, that is, in the presence of a second (adsorptive) species. The process of mediated coadsorption of a molecular species at the liquid−solid interface was accomplished through complexation of TPT with a second type of molecule acting as a "molecular glue" via hydrogen bonds. Scanning tunneling microscopy (STM) was utilized to investigate the structure of the coadsorbed monolayers at the liquid−solid interface. Trimesic acid (TMA) and terephthalic acid (TPA)—both benzene rings with disposed carboxylic acid groups—were appropriate to precipitate the stable adsorption of TPT. According to the different symmetry and number of carboxylic acid groups, various networks were observed.

Introduction

Self-assembled monolayers (SAMs) are an important stepping off point for novel applications of long range ordered organic films in molecular electronics, catalysis, or sensor development. Hence, it is of general interest to understand the parameters determining growth and stability. Generally, the self-assembly process of two-dimensional networks on surfaces is governed by a crucial balance between adsorbate−substrate and adsorbate−adsorbate (either direct or mediated by the substrate) interactions. For weak interacting substrates such as layered materials, the molecule−molecule interactions can become predominant, particularly if hydrogen bonds come into play. However, even for inferior substrate influence, normally there is a distinct relation between adsorbate and substrate lattice, for example, commensurability or point on line structures.[1,2] Hydrogen bonds are of particular interest in 2D self-assembled networks because they are highly selective and directional, though moderately strong.[3−6]

Scanning tunneling microscopy (STM) has proven to be an ideal in situ probe for the structural and electronic properties of the coupled adsorbate−substrate system at the interface between solution and solid.[7,8] In contrast to vacuum deposition experiments, stable adsorption at the liquid−solid interface only occurs if it leads to a minimum in free energy (equilibrium); thus, the molecules have an additional degree of freedom to remain dissolved. For these kinds of experiments, the size of the molecular adsorbates always represents a tradeoff: the larger a molecule is, the larger is its adsorption energy. However, the solubility of the compound normally decreases with increasing size. A common strategy to enhance the adsorption energy of compounds is to append alkyl chains, acting as anchor groups on a graphite surface.[9−11] Since there is an almost perfect registry between the graphite(0001) surface and the alkane backbone, the additional contribution to the adsorption energy increases nearly linearly with chain length, as verified by thermal desorption spectroscopy experiments.[12−14] However, the covalently attached alkane chains alter the molecular structure and can also be used to tailor the monolayer structure, for example, the spacing between lamellae of a porphyrin core.[11] In this work, we implement a different strategy: H-bonds are utilized to create noncovalently bound complexes of 1,3,5-tris(4-pyridyl)-2,4,6-triazine (TPT) and a second type of molecule, which acts as a linker. Because stable adsorption of TPT itself from the liquid phase has never been observed, these complexes facilitate the adsorption through an increased adsorption energy.

Experimental Section

All experiments were conducted at the liquid−solid interface under ambient conditions with a home-built pocket size scanning tunneling microscope driven by a commercial RHK SPM-100 control system. As probes, mechanically cut Pt/Ir tips were used, which were conditioned by short voltage pulses if necessary. Since the solvents used here are electrically nonconducting, it was not necessary to insulate tips.

Samples were prepared by depositing a small droplet (∼5 μL) of solution on the basal plane of freshly cleaved, highly oriented pyrolytic graphite (HOPG). It is noteworthy that the influence of the solvent on the equilibrium between molecules in solution and on the surface can be crucial. By means of the homologous series of fatty acids, it has been shown that a particular modification of a polymorphic adsorption system can be selected by solvent identity.[15] A suitable solvent in this case is heptanoic acid ($CH_3(CH_2)_5COOH$), because the carboxylic group is responsible for dissolving the molecules used herein. Also, the vapor pressure of heptanoic acid is low enough for room temperature STM experiments to be performed for up to 1 h after deposition. Elevated temperatures favor solvent evaporation, significantly shortening the sample's lifetime.

Tunneling voltages between +0.3 and +1.6 V, with respect to the tip, and reference currents around 100 pA were used. All STM images shown were recorded in the constant current mode

* Corresponding author. Phone: +49 89 2180 4188. Fax: +49 89 2180 4334. E-mail: markus@lackinger.org.
[†] Ludwig-Maximilians-University Munich and Center for Nanoscience (CeNS).
[‡] Deutsches Museum.

10.1021/jp050794+ CCC: $30.25
Published on Web 06/30/2005

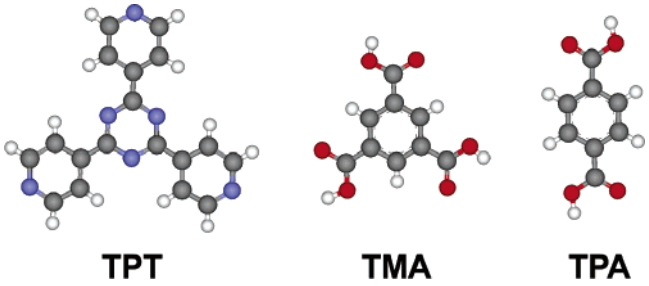

Figure 1. Structures of the adsorbate molecules: 1,3,5-tris(4-pyridyl)-2,4,6-triazine (TPT), trimesic acid (TMA), and terephthalic acid (TPA). In the structures, gray corresponds to carbon atoms, white to hydrogen atoms, red to oxygen atoms, and blue to nitrogen atoms, respectively.

of operation. For noise reduction, the STM images were processed by leveling and 3 × 3 G filtering.

Results and Discussion

We investigate the adsorption behavior of TPT at the liquid−solid interface in the presence of either trimesic acid (TMA) or terephthalic acid (TPA). TPT consists of a triazine ring in the center with three symmetrically disposed pyridyl rings. Similar to TMA and TPA, TPT is a planar molecule (cf. Figure 1). Adsorption with the molecular plane parallel to the substrate is observed for comparable aromatic molecules, thereby optimizing the interaction with the substrate.[16−18] However, despite many attempts, adsorption of TPT from heptanoic acid solution only containing this species has never been observed. In an equilibrated system, TPT molecules remain dissolved and do not form an interfacial monolayer. Stronger interacting substrates, for example, metal surfaces, might possibly shift the equilibrium toward adsorption. Densely packed structures evolve when a monolayer of TPT is evaporated on graphite at room temperature in an ultrahigh vacuum (UHV) environment.[19]

TMA consists of a benzene ring with three carboxylic acid groups symmetrically attached in the 1, 3, and 5 positions. Because of the carboxylic acid groups, TMA and TPA respectively have the ability to form homomolecular H-bonds. Since carboxyl groups are both proton donors and acceptors, they can hydrogen bond with themselves without the necessity of any other functional group.[20] Consequently, both TMA and TPA form H-bond structures at the liquid−solid interface through spontaneous self-assembly.[15,21] In contrast to TPA, TMA assembles on graphite in a loosely packed structure, with ∼1.0 nm wide cavities appropriate for the incorporation of molecular guests.[22,23] A comparable TMA host structure was also observed in an electrochemical STM study on Au(111) under suitable potential conditions[24] and in UHV experiments with TMA submonolayers evaporated on Cu(100).[25] However, another electrochemical STM study of TMA on Au(111) revealed also potential driven phase transitions and various phases with upright molecules.[26] Similarly, TPA monolayers were investigated on Au(111)[27] and Cu(100)[28] by STM under UHV conditions.

Usually, stable adsorption of molecular monolayers at the liquid−solid interface only takes place in an equilibrium situation when the system minimizes free energy. There are at least four significant contributions to the free energy: adsorption energy, solvation energy, intermolecular interaction, and entropy. In many cases, the adsorption energy of just a monomer is not sufficient for the evolution of stable monolayers, particularly for small molecules on weakly interacting substrates such as layered crystals (e.g., graphite). Therefore, strong intermolecular interactions such as H-bonds enhance the stabilization energy for molecules on the surface and can eventually lead to self-assembly of stable monolayers at the interface. In this case, coadsorption of TPT as a proton acceptor together with either TMA or TPA molecules as proton donor leads to stable adsorption of TPT through N···H−O H-bonds. Although the self-assembled networks formed by the two systems are quite different, the same driving force, namely, H-bonds, is evident.

For the systems under investigation, the concentration ratio of both adsorbates can be crucial. Because of the possibility of forming two H-bonds per carboxylic group, TMA and TPA molecules have a high affinity to building networks with themselves rather than mixed networks with TPT molecules. For that reason, we used for the system TPT + TMA a volume ratio of (6 parts of TPT solution):(1 part of TMA solution):(8 parts of solvent), where TPT and TMA solution represent a saturated solution in heptanoic acid. Dilution with pure solvent became necessary because more concentrated solutions lead to the precipitation of presumably bulk cocrystals of TPT and TMA all over the surface, as identified with an optical microscope. In the case of TPT and TPA, preparation was straightforward, since a saturated binary solution of TPT and TPA in heptanoic acid with a sediment of both TPT and TPA worked. The sediment should also contain a phase with the TPT−TPA bulk cocrystal in equilibrium with the liquid phase.

TPT and TMA

The binary solution of TPT and TMA leads to a coadsorbed monolayer with a 6-fold symmetry, as seen in the STM image presented in Figure 2a. Assuming parallel adsorption of both molecules, each can be clearly distinguished by means of their apparent size in the STM image. Single TPT molecules appear as a triangle of elevated circular features with a central depression. This 3-fold symmetry of TPT in the STM contrast agrees with the symmetry of the molecular structure. In addition, the spacing between intramolecular intensity minima of TPT (marked by white arrows in Figure 2a and assigned to the center of pyridyl groups) is ∼0.7 nm and matches the distance predicted by a molecular mechanics simulation of the TPT structure. Similar distances were found for the features assigned to the TPT molecule in the TPT−TPA cocrystal as discussed below. Also, the three grouped features identified as the TPT molecule exhibit similar apparent heights, whereas the single circular protrusion assigned to the TMA molecule (marked by a white circle in Figure 2a) appears remarkably darker. This similarity in intensity provides some evidence that the three grouped features can be assigned to the same molecule, namely, TPT. Furthermore, in the STM contrast appears an undefined structure inside the cavities. This might stem from a transient adsorption of guests (either TMA, TPT, or heptanoic acid molecules). However, their adsorption energy is not large enough to allow for a clear imaging process. Possible explanations comprise that the molecules are either pushed away by the tip or desorb again on a rapid time scale. A model of the assembly structure indicating the H-bonding scheme is depicted in Figure 2b. The honeycomb packing motif of TPT−TMA is already known from X-ray diffraction experiments on bulk cocrystals.[29] In this study a dense packing was inhibited by pyrene guests within the cavities of aligned TPT−TMA honeycomb planes, thereby forming pyrene "nanorods". However, the 2D cocrystal is loosely packed and exhibits a periodic arrangement of voids, which might by suited for the guided coadsorption of a guest within this host network. As mentioned previously, TMA by itself also forms a host system on graphite[20] and molecular guests were already incorporated at the liquid−solid interface.[22,23] The lattice constant of the mixed system is

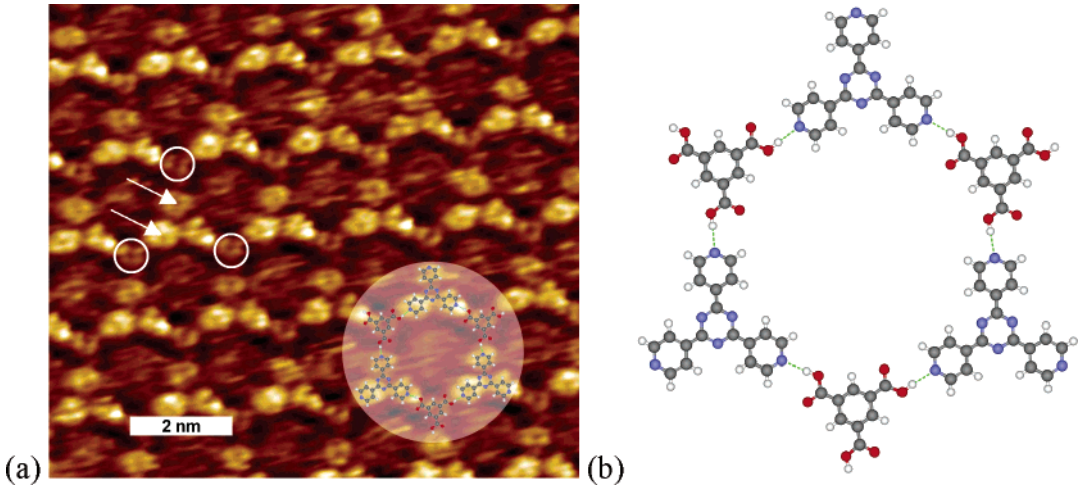

Figure 2. (a) STM topograph of the 2D TPT−TMA cocrystal on HOPG (0001). The white circles indicate TMA molecules, and the arrows mark the center-to-center distance (∼0.7 nm) between two pyridyl groups of one TPT molecule. (b) Molecular model of the structure, where one TMA coordinates three TPT molecules via H-bonds. The cutout shows three TPT molecules and three TMA molecules bordering one cavity of the host network. The dashed lines indicate N···H−O H-bonds.

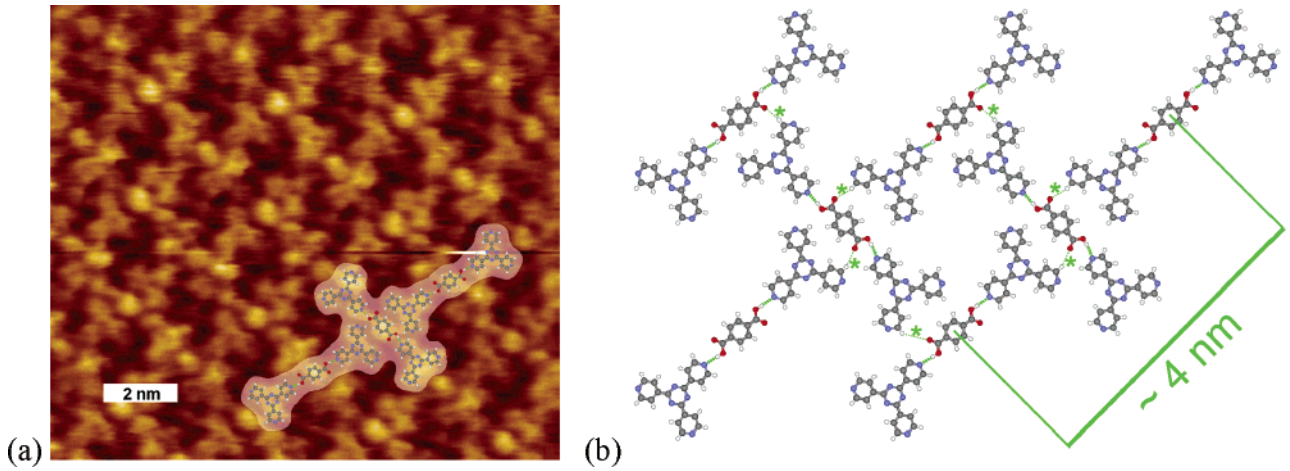

Figure 3. (a) STM topograph of the 80° TPT−TPA cocrystal on HOPG (0001). TPT molecules appear as several bright, triangularly arranged features, whereas TPA appears as a single round feature. (b) Molecular model of the 90° TPT−TPA structure (the bold dashed green lines indicate the N···H−O H-bonds of the TPT−TPA−TPT basic units, and the fine green lines (additionally marked with asterisks) indicate weaker C−H···O H-bonds between these building blocks).

larger than that for pure TMA layers (∼2.0 nm vs ∼1.6 nm), because the TPT molecule is much larger than TMA. Even larger cavities (diameter ∼2.8 nm) could be achieved with benzenetribenzoic acid (BTB) as a building block.[30] The structure of BTB is rather similar to that of TPT but with carboxylic acid groups as linkers at the periphery. Another characteristic of the TPT−TMA system is the free carbonyls of the acid groups of TMA protruding into the cavity. They might serve as sites for H-bonds between the cavity wall and potential guest molecules.

To obtain the crystallographic relation between substrate and adsorbate, that is, the superstructure matrix, the adsorbate and substrate lattices were recorded within one scanning frame, as shown previously for dicarboxylic acids.[21] Fast Fourier transformation (FFT) of those split images allows for a precise determination of the superstructure matrix. By using the graphite lattice as an intrinsic ruler, it was possible to determine the unit cell of the monolayer, thereby excluding external falsifications such as drift or scanner calibration.

$$\begin{pmatrix}\vec{A}\\ \vec{B}\end{pmatrix}=\begin{pmatrix}7 & 9\\ -2 & 7\end{pmatrix}\begin{pmatrix}\vec{a}\\ \vec{b}\end{pmatrix} \text{ or alternatively } \begin{pmatrix}\vec{A}\\ \vec{B}\end{pmatrix}=\begin{pmatrix}9 & 7\\ 2 & 9\end{pmatrix}\begin{pmatrix}\vec{a}\\ \vec{b}\end{pmatrix}$$

The experimental error of the coefficients is in the range ±0.5. This and all following matrices refer to substrate base vectors with an angle of 120°. As the unit cells are rather large, the relative error of the adsorbate vector is still below 7%. According to the commensurate matrix, the length of the adsorbate vectors amounts to 2.01 nm. The angle between the vectors is exactly 60° and thus is consistent with the anticipated 6-fold symmetry of the structure. Both adsorbate vectors are rotated by approximately +12.2° with respect to the graphite lattice. The second matrix was measured as well and describes a symmetry equivalent adsorbate lattice (mirrored on a graphite axis) with an angle of approximately −12.2° to the graphite lattice.

TPT and TPA

The coadsorption of TPT and TPA molecules on HOPG(0001) leads to a comparatively densely packed structure with a bone-shaped packing motif, as seen in the STM image in Figure 3a.

The TPT−TPA network is built up of small hydrogen-bond units, comprised of two TPT molecules interconnected by a TPA molecule (cf. Figure 3b). In this packing motif, the carboxylic hydrogen atoms are bound to the outer nitrogen atoms of TPT

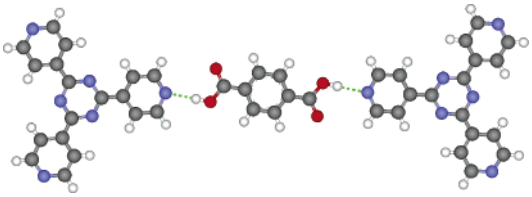

Figure 4. Model of the basic unit of the 2D TPT−TPA crystal consisting of two TPT molecules and one TPA molecule connected via H-bonds. The dashed lines indicate N···H−O H-bonds, and the TPT center-to-center distance amounts to ∼2.5 nm.

via N···H−O H-bonds. This defines the basic unit of the bone-shaped structure, as depicted in Figure 4. The neighboring units are located perpendicular with their axis in the middle of the long axis of the first one, as indicated in Figure 3b. This results in a more or less quadratic weaving pattern of molecules laying length- and crosswise. Referring to the angle between neighboring basic units, two different structures were observed: One structure is quadratic within the experimental error with an angle of 90° between the units, as shown in the model of Figure 3b. The second structure is slightly tilted which results in an angle of ∼80° between the two axes of neighboring basic units. The distance between two equally oriented units is about 4 nm in each direction, as indicated in Figure 3b.

To precisely measure the superstructure matrices, split images with substrate and adsorbate in one frame were recorded. Using FFT and the graphite layer as a reference, the commensurate superstructure matrices of the two TPT−TPA polymorphs were determined:

$$\begin{pmatrix}\vec{A}\\ \vec{B}\end{pmatrix} = \begin{pmatrix}8 & 0\\ 5 & 10\end{pmatrix}\begin{pmatrix}\vec{a}\\ \vec{b}\end{pmatrix} \text{ (90° structure) and}$$

$$\begin{pmatrix}\vec{A}\\ \vec{B}\end{pmatrix} = \begin{pmatrix}10 & 5\\ 1 & 9\end{pmatrix}\begin{pmatrix}\vec{a}\\ \vec{b}\end{pmatrix} \text{ (80° structure)}$$

It is reasonable to assume that both structures do not exhibit a significant difference in total free energy, an observation which is generally made for polymorphic modifications. For a comprehensive study of the binding energy, calculations, which use the measured unit cell parameters as a constraint, are highly desirable. However, the accuracy of molecular mechanics simulations might not be sufficient to unambiguously reveal small differences (in comparison to the thermal energy) in total energy.

Both the TPT−TMA and the TPT−TPA cocrystals are stabilized by N···H−O H-bonds, and all carboxylic acid groups of either TMA or TPA participate in the H-bonding. The main difference between TPT−TMA and TPT−TPA coadsorption structures is the H-bond networking. In the TPT−TMA structure, all outer nitrogens of TPT are involved in H-bonds, resulting in an actual network. However, for TPT−TPA, only the basic unit—comprised of two TPT molecules and one TPA molecule—is strongly H-bonded. These units interact and assemble through comparatively weak van der Waals bonds. However, additional C−H···O H-bonds between the hydrogen atoms of TPT and the carboxylic oxygen atoms of TPA, as indicated in Figure 3b, might additionally stabilize that structure. The distance between the corresponding carbon and oxygen atoms (∼0.4 nm) as evaluated from the scaled models matches the range for C−H···O bonds (0.3−0.4 nm in a straight configuration).[31] Although this kind of H-bond is comparatively weak, its stabilizing influence exceeds exclusive van der Waals bonding. In all structures, both TPA and TMA coordinate as many TPT molecules as there are carboxylic acid groups available.

The binding energy for TMA is presumably larger than that for TPA, since it forms three H-bonds versus two for TPA, while both molecules have an aromatic system of equal size. The binding energy of a single N···H−O bond was determined in molecular mechanics simulations, with a Dreiding II force field[32] containing a specific term for H-bonds. It was calculated as the difference in binding energies of a TMA molecule bound to a TPT molecule on graphite and a TMA molecule and a TPT molecule bound to the substrate only without intermolecular interaction (H-bond energy = $[\text{TMA}\cdots\text{TPT}]_{\text{HOPG}} - [\text{TMA}]_{\text{HOPG}} - [\text{TPT}]_{\text{HOPG}}$). It amounts to 0.17 eV versus ∼0.30 eV for a 2-fold H-bond among two carboxylic acid groups. Thus, it is a weaker H-bond but nevertheless still sufficient to mediate the stable adsorption of TPT at the liquid−solid interface.

Conclusion

The possibility of precipitating stable adsorption of TPT from the liquid phase through H-bond linker molecules, namely, TMA or TPA, was demonstrated. In the absence of coadsorbates, the stabilization energy of TPT on a graphite surface is not sufficient to observe adsorption from heptanoic acid solution in situ by STM. However, in binary solutions with either TMA or TPA, the second species enables self-assembly of mixed networks on the surface. Intermolecular N···H−O H-bonds are the predominant interaction and thus the driving force for the self-assembly process. When using the 3-fold symmetric TMA as "molecular glue", a hexagonal structure was observed. However, with the 2-fold symmetric TPA molecule, two slightly different structures were revealed, one of them being quadratic.

The TPT−TMA system can be considered a 2D molecular host system with chemically reactive walls. These walls offer free carbonyls of TMA that protrude into the cavity, as binding sites for potential guests. This system might be suitable for immobilizing further species, enabling spectroscopic measurements without requiring low temperatures or strongly interacting substrates, which may interfere with the object under investigation. By combining two different entities in tailored supramolecular structures, a greater variety of properties can be achieved, which increases the benefits and chances for future applications. For that reason, it is an interesting and challenging goal to investigate the conditions for 2D self-assembly of mixed networks.

Acknowledgment. The authors would like to thank Dr. Gina Florio for valuable discussions and proofreading and Dr. Ferdinand Jamitzky for molecular mechanics simulations. The financial support of the Deutsche Forschungsgemeinschaft (DFG) within the SFB 486 is gratefully acknowledged.

References and Notes

(1) Cyr, D. M.; Venkataraman, B.; Flynn, G. W. *Chem. Mater.* **1996**, *8*, 1600.

(2) Jonkheijm, P.; Hoeben, F. J. M.; Kleppinger, R.; van Herrikhuyzen, J.; Schenning, A. P. H. J.; Meijer, E. W. *J. Am. Chem. Soc.* **2003**, *125*, 15941.

(3) Jeffrey, G. A. *An introduction to hydrogen bonding*; Oxford University Press: New York, Oxford, U.K., 1997.

(4) De Feyter, S.; De Schryver, F. C. *Chem. Soc. Rev.* **2003**, *32*, 139.

(5) Yokoyama, T.; Yokoyama, S.; Kamikado, T.; Okuno, Y.; Mashiko, S. *Nature* **2001**, *413*, 619.

(6) Theobald, J. A.; Oxtoby, N. S.; Phillips, M. A.; Champness, N. R.; Beton, P. H. *Nature* **2003**, *424*, 1029.

(7) Claypool, C. L.; Faglioni, F.; Goddard, W. A.; Gray, H. B.; Lewis, N. S.; Marcus, R. A. *J. Phys. Chem. B* **1997**, *101*, 5978.

(8) Giancarlo, L. C.; Flynn, G. W. *Acc. Chem. Res.* **2000**, *33*, 491.

(9) De Feyter, S.; Gesquiere, A.; Abdel-Mottaleb, M. M.; Grim, P. C. M.; De Schryver, F. C.; Meiners, C.; Sieffert, M.; Valiyaveettil, S.; Mullen, K. *Acc. Chem. Res.* **2000**, *33*, 520.

(10) Eichhorst-Gerner, K.; Stabel, A.; Moessner, G.; Declerq, D.; Valiyaveettil, S.; Enkelmann, V.; Müllen, K.; Rabe, J. P. *Angew. Chem., Int. Ed.* **1996**, *35*, 1492.

(11) Wang, H. N.; Wang, C.; Zeng, Q. D.; Xu, S. D.; Yin, S. X.; Xu, B.; Bai, C. L. *Surf. Interface Anal.* **2001**, *32*, 266.

(12) Paserba, K. R.; Gellman, A. J. *J. Chem. Phys.* **2001**, *115*, 6737.

(13) Paserba, K. R.; Gellman, A. J. *Phys. Rev. Lett.* **2001**, *86*, 4338.

(14) Müller, T.; Flynn, G. W.; Mathauser, A. T.; Teplyakov, A. V. *Langmuir* **2003**, *19*, 2812.

(15) Lackinger, M.; Griessl, S.; Heckl, W. M.; Hietschold, M.; Flynn, G. W. *Langmuir* **2005**, *21*, 4984−4988.

(16) Lu, X.; Hipps, K. W. *J. Phys. Chem. B* **1997**, *101*, 5391.

(17) Lackinger, M.; Müller, T.; Gopakumar, T. G.; Müller, F.; Hietschold, M.; Flynn, G. W. *J. Phys. Chem. B* **2004**, *108*, 2279.

(18) Toerker, M.; Fritz, T.; Proehl, H.; Sellam, F.; Leo, K. *Surf. Sci.* **2001**, *491*, 1.

(19) Kampschulte, L. Unpublished observation, 2005.

(20) Griessl, S.; Lackinger, M.; Edelwirth, M.; Hietschold, M.; Heckl, W. M. *Single Mol.* **2002**, *3*, 25.

(21) Lackinger, M.; Griessl, S.; Markert, T.; Jamitzky, F.; Heckl, W. M. *J. Phys. Chem. B* **2004**, *108*, 13652.

(22) Griessl, S.; Lackinger, M.; Jamitzky, F.; Markert, T.; Hietschold, M.; Heckl, W. M. *Langmuir* **2004**, *20*, 9403.

(23) Griessl, S. J. H.; Lackinger, M.; Jamitzky, F.; Markert, T.; Hietschold, M.; Heckl, W. M. *J. Phys. Chem. B* **2004**, *108*, 11556.

(24) Ishikawa, Y.; Ohira, A.; Sakata, M.; Hirayama, C.; Kunitake, M. *Chem. Commun.* **2002**, 2652.

(25) Dmitriev, A.; Lin, N.; Weckesser, J.; Barth, J. V.; Kern, K. *J. Phys. Chem. B* **2002**, *106*, 6907.

(26) Su, G. J.; Zhang, H. M.; Wan, L. J.; Bai, C. L.; Wandlowski, T. *J. Phys. Chem. B* **2004**, *108*, 1931.

(27) Clair, S.; Pons, S.; Seitsonen, A. P.; Brune, H.; Kern, K.; Barth, J. V. *J. Phys. Chem. B* **2004**, *108*, 14585.

(28) Stepanow, S.; Strunskus, T.; Lingenfelder, M.; Dmitriev, A.; Spillmann, H.; Lin, N.; Barth, J. V.; Woll, C.; Kern, K. *J. Phys. Chem. B* **2004**, *108*, 19392.

(29) Ma, B. Q.; Coppens, P. *Chem. Commun.* **2003**, 2290.

(30) Griessl, S.; Lackinger, M.; Maier, A.-K.; Kishore, R. S. K.; Kampschulte, L.; Schmittel, M.; Heckl, W. M. *Chem.—Eur. J.*, submitted for publication, 2005.

(31) Desiraju, G. R. *Acc. Chem. Res.* **1996**, *29*, 441.

(32) Mayo, S. L.; Olafson, B. D.; Goddard, W. A., III. *J. Phys. Chem.* **1990**, *94*, 8897.